ACS OMEGA

http://pubs.acs.org/journal/acsodf

Article

Storage and Temperature Stability of Emulsified Biodiesel−Diesel Blends

Nitai C. Maji, Preetika Rastogi, Anand Krishnasamy, Indrapal Singh Aidhen, Niket S. Kaisare,* and Madivala G. Basavaraj*

Cite This: *ACS Omega* 2022, 7, 44762−44771

Read Online

ACCESS | Metrics & More | Article Recommendations

ABSTRACT: The scarcity of fossil fuel has led to the recent worldwide commercialization of biodiesel-blended diesel. The benefits associated with emulsion fuels have encouraged researchers to study the blended emulsified fuels in diesel engines. Recent results show the effectiveness of blended emulsified fuels in terms of better fuel economy and less harmful emissions. Investigation on the stability of these blended emulsified fuels during storage in the fuel tank is equally crucial for commercialization and practical application. A systematic study on the storage stability of water in biodiesel/diesel blend nanoemulsions (nEs) is presented in this work. A mixture of two biodegradable surfactants, Span 80 and Tween 80, is used to stabilize the nEs. The nEs are formulated by subjecting a mixture of 5 vol % of each surfactant, 5 vol % of water, and 85 vol % of pure or blended diesel to high shear homogenization at 5000 rpm for 2 min. Storage stability of the emulsified fuels is studied for 65 days at 25 °C with the help of dynamic light scattering and viscosity measurements. The mean droplet size increases, and the stability decreases with an increase in the biodiesel concentration. The smallest mean droplet size is 32 nm for emulsified fuel using pure diesel, and these emulsions remain stable for 65 days. No macroscopic phase separation is observed for any sample aged for 24 days. A moderate increment in droplet sizes is observed during this period. The droplet size increases significantly when more than 15 vol % biodiesel is used in the fuel blend. Those samples show stratification after 65 storage days. An increment in the zero-shear viscosity of the samples over aging helps hinder the rapid coalescence of the droplets, thus preventing phase separation. Furthermore, the thermal stability of the samples is also investigated at elevated temperatures up to 50 °C. The nEs are found to be highly stable within this temperature range and showed a moderate change in mean droplets size, especially when the concentration of biodiesel in the emulsified fuel blend is less than 15 vol %.

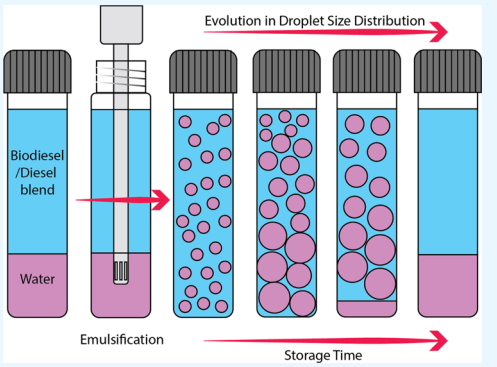

1. INTRODUCTION

Diesel engines are efficient and cost-effective power sources utilized in various industries, including locomotive, construction, and agriculture.[1,2] Due to the depletion of fossil fuels and the need to reduce hazardous emissions (unburned hydrocarbons, CO, NO_x, and particulate matter) from diesel engines, alternate fuel sources are being explored.[3] Biodiesel, which consists of mono-alkyl esters of long-chain fatty acids generated from vegetable oil and animal fats, is a prospective alternative as a clean fuel. Biodiesel having higher oxygen content and lower heating value reduces the formation rate of CO, unburned hydrocarbon, and particulate matter.[4] There are conflicting claims on NO_x emissions when biodiesel is used as fuel for powering internal combustion engines. Some literature claims that biodiesel increases NO_x emissions,[5] while other claims it reduces NO_x emissions (the consensus is higher NO_x emissions with biodiesel).[6] The shortage of conventional fossil fuels has intensely diverted attention toward the commercialization of diesel blended with 5−20% biodiesel in the world market.[7]

High combustion temperature results in a higher NO_x formation rate according to the well-accepted Zeldovich mechanism, and it may increase further by higher oxygen content in biodiesel.[4] Hence, there are efforts to reduce combustion temperature by introducing water into the combustion chamber. Some standard methods are injecting water directly into the cylinder by the electronic fuel injection system[8] or fumigation,[3] where steam is mixed with the intake air. However, these methods have limitations; for example, a hydrostatic lock can occur when the piston comes in contact

Received: July 26, 2022
Accepted: October 26, 2022
Published: December 2, 2022

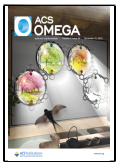

with water at its minimum volume position. Moreover, water can adversely affect engine system components under cold climate conditions. This may further result in corrosion and physical damage to the engine system components upon prolonged use.[3] Water emulsified fuel is another efficient approach for increasing the thermal efficiency and lowering combustion temperature and pollutant emission. This method is less prone to corrosion than other methods and does not require any hardware modifications to the existing diesel engine.[9] Emulsified fuel is a biphasic dispersion of polar water dispersed in nonpolar fuels such as diesel. The presence of water droplets in the fuel leads to micro explosions during combustion,[10] which helps burn the fuel efficiently as it leads to a more uniform distribution of the fuel inside the combustion chamber. Surfactants are used to lower the interfacial tension between immiscible liquids (fuel and water) and help in stabilizing the droplets of the dispersed phase by preventing coalescence. Emulsified fuels with less than 1 μm droplets have attracted substantial consideration from the fuel research groups for excellent stability against aggregation and gravitational separation. Nanoemulsions (nEs) are kinetically stable dispersions with droplet sizes of the order of 100 nm. Storage stability of nEs is significantly superior to emulsions of micron to millimeter size droplets but inferior to the thermodynamically stable microemulsions with sub-100 nm droplets.[11] However, nEs are receiving attention due to the requirement for lower concentrations of expensive surfactants.[11]

Recently, Patidar and Raheman[8] investigated the combustion performance and emissions of diesel with a 20% biodiesel blend and water−emulsified blend by performing engine experiments for 100 h. They reported a reduction in NO_x emission and soot deposition by 13.8 and 16.4%, respectively, due to the use of emulsified blends. Maawa et al. also reported a 26.17% reduction in NO_x emission without any change in the engine performance by using a 30% water-emulsified diesel−biodiesel blend.[4] Other researchers observed similar results using nE fuels in conventional diesel engines, including an increase in the brake thermal efficiency and brake specific fuel consumption and a reduction in exhaust gas temperature.[7,12] About 4.84 and 4.65% improvements in diesel engines' power and torque have been reported when nE fuel is used instead of emulsified fuel with larger water droplets.[13]

Comprehensive studies have been carried out on the performance of engines using neat fuels, blended fuels, and blended emulsified fuels. Notwithstanding, investigations on the storage stability of these emulsified fuels are sparse in the literature. The stability of emulsions throughout storage, transit, and operation should be given due consideration for emulsified fuel commercialization. Controlling the water droplet size distribution (DSD) in fuel emulsions is vital for the flow characteristics and storage stability. Basha and Anand reported the stability of mixed surfactant stabilized water in diesel emulsions after adding alumina nanoparticles for 6 days.[14] They observed a reduction in emulsion height from the 2nd day of storage, which reduced to 85% after 6 days. The kinetic stability of mixed surfactant stabilized water in pure diesel emulsions and nE over a more extended storage period of 7 and 50 days, respectively, has been reported.[15] A rapid increase in mean droplet size and sedimentation was observed for prolonged storage. It is also possible to formulate microemulsion fuels that exhibit outstanding storage stability.[16] Christensen and McCormick studied the long-term storage stability of biodiesel and blends.[17] Their results suggest that exposure to water, oxygen, and light contributes to the degradation of the blended biodiesel fuel. Considering the prospects of using biodiesel blends in engines, a systematic study on the storage stability of surfactant stabilized blend-emulsified fuel is inevitable.

The present study describes the formulation of diesel/biodiesel blend nE fuels containing 5 vol % water. An equal volume of mixed surfactant (Span 80 and Tween 80) of 10 vol % is used to stabilize the nEs. Furthermore, a systematic study is presented on the long-term storage stability of these blend-emulsified fuels, and the effect of aging and temperature is discussed based on the change in different physical properties such as density, viscosity, and droplet size.

2. EXPERIMENTAL SECTION

2.1. Materials. Commercial grade diesel was procured from a local Indian oil gas station in Velachery, Chennai, India. Sunflower oil-based biodiesel was purchased from M/s. Mirai Research Solutions, Chennai, India. Deionized (DI) water (18.2 MΩ cm resistivity), obtained from a laboratory water purification system (Milli-Q, Millipore, USA), was used for all the experiments. Sorbitan monooleate (Span 80) and polyoxyethylene sorbitan monooleate (Tween 80) were purchased from Sisco Research Laboratories Pvt. Ltd., India, and Merck, India, respectively. Unless otherwise specified, all the reagents and materials were used as received without further purification.

2.2. Concentration of Span 80 and Tween 80 for Stabilizing nEs. The surfactant with a strong affinity for polar liquids such as water is hydrophilic. In contrast, the surfactant with a strong affinity toward nonpolar liquids such as diesel or biodiesel is lipophilic. The hydrophilic−lipophilic balance (HLB) is a numerical number that ranges from 0 to 20 for a given surfactant or mixture of surfactants. It signifies the quantity of hydrophilic components in the surfactant. A mixture of hydrophilic and lipophilic surfactants has been considered as an efficient stabilizer for water in diesel emulsion.[12,18] An equal volume mixture of Span 80 and Tween 80 is used in this study to stabilize nEs with pure fuel and blends. The properties of both the surfactants are shown in Table 1. The HLB of the mixed surfactant used in this study, calculated as mass-averaged HLB of individual components, is 9.89. As per our previous study,[15] this composition with a total surfactant concentration of 10 vol % efficiently stabilizes water in diesel nEs with 5 vol % water.

Table 1. Properties of Surfactants

surfactant	HLB	density [kg/m^3]	molecular weight [g/mol]
Span 80	4.3	986	428.59
Tween 80	15	1080	1309.63

2.3. Preparation of Emulsified Fuels. Diesel−biodiesel blends were prepared by adding the required amount of biodiesel into pure diesel, followed by magnetic stirring at 1000 rpm for 15 min. Diesel−biodiesel blends, hereafter, will be mentioned as "fuel blends." Fuel blends were stored undisturbed for another 30 min to reach equilibrium. Pure diesel (B0) and fuel blends (B5 to B25) are used as the oil phase to prepare the emulsified fuels. "B" denotes the biodiesel, with the number that follows indicating the volume percentage of biodiesel used to prepare the fuel blend. The water content

https://doi.org/10.1021/acsomega.2c04711
ACS Omega 2022, 7, 44762−44771

in the overall emulsion was kept fixed at 5 vol %. Span 80 and Tween 80 were added in equal volume by keeping the total surfactant concentration constant at 10 vol %. The volumes of individual constituents were converted to mass by knowing their density, and the appropriate quantity of constituents was weighed to prepare different solutions. First, Span 80 was dissolved in the oil phase (diesel or fuel blend) in a pyrex bottle. Later, Tween 80 was added and stirred until a clear solution was obtained. Then, DI water was added to this solution. The entire contents of the bottle were emulsified at room temperature using a homogenizer/disperser (T25 digital ULTRA-TURRAX, IKA, Germany) with S25N-18G dispersing element. The homogenizer works on the principle of rotor-stator assembly with a rotor element of 12.7 mm rotating at high speed inside a stator element of 18 mm. A small gap between the rotor and stator produces powerful shear force, resulting in better dispersion. The samples were homogenized at 5000 rpm for 2 min to obtain water-in-fuel nEs. Compositions of emulsified fuels are shown in Table 2.

Table 2. Composition of Blends and Emulsified Fuels

emulsified fuels	fuel blends (oil)	volume of diesel (%)	volume of biodiesel (%)	volume of Span 80 (%)	volume of Tween 80 (%)	volume of water (%)
B0-nE	B0	85	0	5	5	5
B5-nE	B5	81.75	3.25	5	5	5
B10-nE	B10	76.5	8.5	5	5	5
B15-nE	B15	72.25	12.75	5	5	5
B20-nE	B20	68	17	5	5	5
B25-nE	B25	63.75	21.25	5	5	5

2.4. Study on Storage and Thermal Stability of Emulsified Fuels. The influence of storage time on the stability and nanostructure of emulsified fuels was investigated by storing emulsified fuel samples at 25 ± 0.5 °C in multiple 4 mL vials. The emulsified fuel in the vials was selected randomly after a specific storage time to characterize the evolution of droplet size and viscosity. Furthermore, the thermal stability of the emulsified fuels was studied by storing freshly prepared emulsified fuel samples at an elevated temperature for 2 h in a circulatory water bath (F12-MA, Julabo, Germany). Thermal stability was studied at five different temperatures in the 20−50 °C range.

2.5. Characterization. The density of the samples was measured using an automatic oscillating *U*-tube density meter (DMA 4500 M, Anton-Paar GMBH, Austria). The accuracy of the density measurements is in the range of 0.00005 g/cc. The viscosity measurements were carried out in an automatic micro viscometer (Lovis 2000 ME, Anton-Paar GMBH, Austria) using the rolling ball method in a glass capillary tube of 1.59 mm diameter capable of measuring viscosity up to 20 mPa·s. The instrument was calibrated using DI water before measurements. The viscosity of samples of higher viscosities was measured with a stress and strain-controlled rheometer (MCR 301, Anton Paar, Austria) equipped with a cone-plate geometry with a cone angle of 0.994° and a diameter of 24.98 mm. Experiments were carried out at low shear rates (less than 1 s^{-1}) to measure the zero-shear viscosity (ZSV) of the samples. The refractive index (RI) of diesel and biodiesel−diesel blends was measured using an automatic refractometer (J357, Rudolph Research Analytical, USA). The instrument uses an incident light of 589.3 nm wavelength and has a resolution of ±0.00001 with an accuracy of ±0.00002. The RI of the samples is needed to calculate the size of the droplets from dynamic light scattering (DLS). The flash points of the samples were measured using the ASTM D93 method in an automated Pensky Martens flash point analyzer (AutoFlash-93, Acute Instruments, India). The higher heating values (HHVs) or gross calorific values (GCVs) of the samples were determined using a bomb calorimeter (C2000, IKA, Germany). The photographs of the glass vials containing emulsified fuels were captured using a digital cellphone camera (64-megapixel Samsung GW1 sensor with 0.8 μm pixels and f/1.9 aperture) to visually assess their macroscopic phase behavior or separation.

2.5.1. GC−MS Analysis of Diesel and Biodiesel. Diesel and biodiesel are multicomponent fluids containing mixtures of several aromatic and aliphatic compounds. The biodiesel used for this study is a fatty acid methyl ester obtained from Sunflower oil with 1.41% free fatty acid and 0.02% moisture content, as per the information provided by the manufacturer. Furthermore, the chemical composition of diesel and biodiesel was investigated using a gas chromatography (GC)/mass spectrometry (MS) system (GC-2010 Plus/QP2020, Shimadzu, Singapore) equipped with a DB-5MS capillary column (30 m length × 0.25 mm i.d. × 0.25 μm film thickness). Helium (99.9995%) was used as the carrier gas at a 1.49 mL/min flow rate. The column temperature was maintained at 45 °C for 1 min, then ramped up to 250 °C at 5 °C/min, and held at 250 °C for 20 min. The interface and MS ion source temperatures were set at 300 and 250 °C, respectively. The primary 10 compounds for both diesel and biodiesel are presented in Table 3.

Table 3. Major Components in Diesel and Biodiesel with Area % Obtained from GC/MS

fuel	compounds	area (%)
biodiesel	9-octadecenoic acid (*Z*)-, methyl ester	33.62
	9,12-octadecadienoic acid (*Z*,*Z*)-, methyl ester	29.9
	hexadecanoic acid, methyl ester	12.96
	methyl stearate	6.56
	hexadecadienoic acid, methyl ester	2.64
	9-octadecenoic acid, methyl ester, (*E*)-	2.47
	9-hexadecenoic acid, methyl ester, (*Z*)-	1.3
	oxiraneoctanoic acid, 3-octyl-, methyl ester, *cis*-	1.22
	docosanoic acid, methyl ester	1.09
	11-eicosenoic acid, methyl ester	1.04
diesel	eicosane	12.66
	hexadecane	7.71
	heneicosane	6.77
	heptadecane	3.9
	tetradecane	3.32
	tridecane	2.42
	hexadecane, 2,6,10,14-tetramethyl-	2.36
	pentadecane, 2,6,10,14-tetramethyl-	2.14
	undecane	2.12
	nonane	1.9

2.5.2. Analysis of DSD by Dynamic Light Scattering. Due to its non-invasive nature, the DLS technique is widely used for in situ droplet size measurements in nEs. The technique relies on the measurement of time-dependent fluctuation of scattered light at a fixed scattering angle. In this study, DLS measurements are performed using a nanoparticle size analyzer

https://doi.org/10.1021/acsomega.2c04711
ACS Omega 2022, 7, 44762−44771

(SZ-100 NanoPartica, Horiba, Japan). The sample is placed in a four-side transparent quartz cuvette cell of 3.5 mL volume and 1 cm path length. The sample temperature is maintained by a Peltier heating module attached to the instrument. The equipment uses a diode-pumped solid-state laser (10 mW, Class I) of wavelength 532 nm as a light source. The scattered field takes the shape of a speckle pattern upon irradiating the sample with the laser beam due to the interference of light scattered by droplets in the dispersion. The characteristic time-dependent fluctuations of the scattered intensity are recorded by the photodetector placed at scattering fixed angles such as 90 or 173°. Measured intensity fluctuations are fed into a correlator, which generates an intensity correlation function with delay time. The mean size and the size distribution of the droplets can be determined by analyzing the correlation function.

The intensity time correlation function $[g^2(\tau)]$, obtained from the correlator, is converted to the electric field correlation function $[g^1(\tau)]$, which generally follows a single exponential decay for a spherical monodispersed system. For polydisperse systems, which is typically the case for emulsions prepared by high energy homogenization, the decay of the electric field autocorrelation function may be represented as a cumulative sum or integral of the exponential decay function. This function can be expressed mathematically as

$$g^1(\tau) = \int_0^\infty G(\Gamma)\exp(-\Gamma\tau)\mathrm{d}\Gamma \tag{1}$$

with

$$\int_0^\infty G(\Gamma)\mathrm{d}\Gamma = 1 \tag{2}$$

where $\Gamma = Dq^2$ is the decay rate for the droplets of a specific size, D is the translational diffusivity, and q is the scattering vector expressed as $(4\pi n/\lambda)\sin(\theta/2)$, n is the RI of the continuous fuel phase, λ is the wavelength of the laser, θ is the scattering angle, and $G(\Gamma)$ is the decay rate distribution, which is normalized to one (eq 2).

The cumulant method is generally used to analyze the size distribution of a dispersed phase with low polydispersity.[19] In this method, $\exp(-\Gamma\tau)$ term in eq 1 is expanded about a mean value $(\bar{\Gamma})$. By neglecting the higher-order terms for a relatively narrow distribution of $G(\Gamma)$, we get

$$\ln[g^1(\tau)] = \ln B - \bar{\Gamma}\tau + \frac{\mu_2\tau^2}{2} \tag{3}$$

The mean size $(\bar{\Gamma})$ and the variance (μ_2) are obtained by fitting $\ln[g^1(\tau)]$ to a quadratic function of τ. The polydispersity index (PI) is determined by $\mu_2/\bar{\Gamma}^2$. However, for a general polydisperse system with a PI of more than 0.1,[20] an inverse Laplace transform of $g^1(\tau)$ is carried out to obtain $G(\Gamma)$ from eq 1. However, this problem is mathematically ill-posed.[21] A slight disturbance in the correlation data results in a significant error in the obtained particle size distribution. CONTIN algorithm is used to minimize this error and get a closely accurate solution for eq 1.[21] It uses a regularized non-negative least square method.[20,22] In this method, $\chi^2(\alpha)$ given by eq 4 is minimized

$$\chi^2(\alpha) = \sum_{i=1}^{N} \|G(\Gamma)\exp(-\Gamma\tau_i) - g^1(\tau_i)\|^2 + \alpha^2 \left\| \frac{d^2G(\Gamma)}{\mathrm{d}\Gamma^2} \right\|^2 \tag{4}$$

where α is the regularization parameter and the second derivative of $G(\Gamma)$ or the curvature of $G(\Gamma)$ is taken as the operator of the regularization. The first term on the right-hand side of eq 4 refers to the conventional residual norm, and the second term refers to the regularized side constraint. In the present study, a MATLAB code is used to perform CONTIN analysis. It is an emulated version of Provencher's FORTRAN code.[21,23] The value of α need to be taken very carefully. When α is large, the residual norm becomes very large compared to the small side constraint term, and for small α values, the side constraint becomes large compared to the small residual norm. The L-Curve method helps in optimizing the value of α, which provides a best-fitted solution for this kind of ill-posed problem.[22] The goal is to invert the correlation data using CONTIN algorithm for different α-values and calculate the solution norm $(\|G(\Gamma)\|^2)$ and the residual norm. Then, solution norm and residual norm are plotted on a log−log scale. An L-shaped curve is obtained with a characteristic corner dividing a vertical and horizontal branch. This characteristic corner corresponds to the optimum value of α. Then, decay rate distribution, $G(\Gamma)$, is obtained for the optimum α. Finally, the hydrodynamic diameter (d_h) of the droplets corresponds to Γ, which is obtained using the Stoke-Einstein equation

$$d_h = \frac{k_B T}{3\pi\mu D} = \frac{k_B T q^2}{3\pi\mu\Gamma} \tag{5}$$

where k_B is the Boltzmann constant, T is the absolute temperature, and μ is the dynamic viscosity of the dispersion.

3. RESULTS AND DISCUSSION

3.1. Flash Point and Heating Value of Pure and Emulsified Fuels. The flash point of the fuel is the lowest temperature at which the volatile components vaporize to form an ignitable mixture.[24] It is a vital fuel property that determines its effectiveness. Flash points and HHVs of the pure and emulsified fuels are shown in Table 4. It is observed that the flash point of emulsified fuels is not significantly altered from that corresponding to pure diesel. The flash point of nEs increased with the increasing biodiesel content, with only a modest increase to 53.6 °C for B25-nE compared to neat diesel (50.4 °C). Since diesel has the most volatile components

Table 4. Flash Points and HHVs for Pure and Emulsified Fuels

fuel	flash point (°C)	HHV (MJ/kg)
Diesel	50.4	43.9
Biodiesel	163.2	37.3
B0-nE	49.1	41.9
B5-nE	51.1	41.2
B10-nE	51.2	40.5
B15-nE	51.6	40.4
B20-nE	52.8	39.9
B25-nE	53.6	39.4

https://doi.org/10.1021/acsomega.2c04711
ACS Omega 2022, 7, 44762−44771

among the other constituents of the emulsified fuel, it vaporizes first and ignites at around the same temperature (flash point).

A HHV or GCV estimates the energy density of the fuel. It measures the gross amount of heat energy produced upon complete combustion of 1 kg of fuel. HHV of the diesel is found to be the highest, while that of biodiesel is found to be the lowest among the samples, which is consistent with literature reports.[25] All emulsified fuels possess an intermediate HHV. A maximum reduction of 10% in HHV is observed in B25-nE compared to pure diesel. Hence, the energy density of these emulsified fuels is in the range acceptable for engine applications.

3.2. Storage Stability of Emulsified Fuels Based on the Evolution of Droplet Size. The primary processes that lead to destabilization of w/o emulsions are sedimentation, creaming, flocculation, and Ostwald ripening.[26] The dispersed phase droplets coalesce and form two separate liquid layers based on their relative density. Moreover, bigger droplets settle down to the bottom of the storage vessel, resulting in size-dependent segregation of droplets along the depth of the storage vessel. Hence, the dispersion stability of the emulsified fuels can be visualized by observing any stratification in storage vials due to inhomogeneity in droplet sizes. Photographs of the glass vials containing emulsified fuels after different storage times are shown in Figure 1. The turbidity of the emulsified fuels is found to increase with an increase in the biodiesel concentration. In general, opacity signifies the formation of larger-sized drops due to coalescence.[27] At higher biodiesel concentration, a slight increase in opacity is observed with aging. However, no stratification or phase separation is observed for a storage period of 65 days except for B20-nE and B25-nE. No visible phase separation was observed in the initial 24 days for B20-nE and B25-nE; these samples became turbid, and stratification is prominently visible upon storing these emulsified blends over 2 months (as shown in Figure 1f after 65 days of storage).

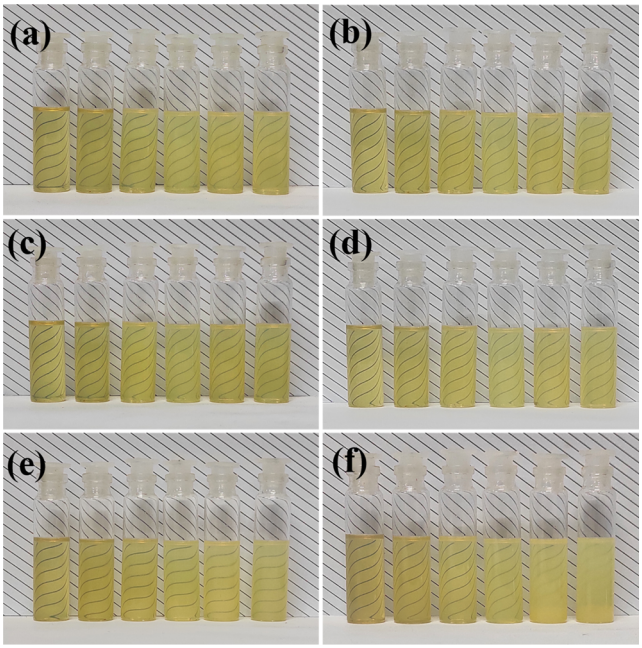

Figure 1. Photographs of emulsified fuels after storing it for (a) 0 day, (b) 1 day, (c) 5 days, (d) 11 days, (e) 24 days, and (f) 65 days. Six vials containing B0-nE, B5-nE, B10-nE, B15-nE, B20-nE, and B25-nE, respectively.

Although there is no macroscopic phase separation (visible to the naked eye) in the samples for up to 24 days, the possibility of stratification, that is, variation in DSD along the height of the storage vials cannot be ruled out. Hence, samples were withdrawn from the top and the bottom of the vials, and DLS measurements were performed. The DSDs obtained from the CONTIN analysis are shown in Figure 2, where the ordinate represents an intensity-weighted normalized function of hydrodynamic diameter (d_h). The freshly prepared samples are stable. DSDs on the first day (storage time = 0 day) for the sample drawn from the top and bottom of the vial are the same regardless of the concentration of biodiesel (as shown in Figure 2). B0-nE has a mean droplet size of 32 nm on day 1. It is highly stable and exhibits a marginal increase in the mean size of approximately 8 nm after 65 days of storage (Figure 2a). In our previous report,[15] we have shown that the mean droplet size of the water in diesel nE increased from 159 to 329 nm over 50 storage days. The modified emulsification method presented in this study enables the preparation of a stable nE with sub-100 nm diameter droplets. The nEs prepared with blended fuel, especially at higher biodiesel content, are less stable as the DSD significantly increases upon storage. The mean droplet size gradually changes from 60 to 90 and 110 nm after 65 days for B5-nE and B10-nE, respectively (Figure 2b,c). No significant difference is observed in DSD at the top and bottom of the vials, pointing to the absence of any stratification. The nEs prepared with blend fuels show bimodal or multimodal distribution. The peaks corresponding to 10 nm size are possibly due to the reverse micelles formed by Span 80 and Tween 80, which are known to be of about 10−20 nm size range.[28] Furthermore, CONTIN analysis can yield false peaks in the distribution function at d_h < 10 nm. Hence, it is challenging to infer whether these peaks around 10 nm are tiny droplets or reverse micellar structures.

From the data presented in Figures 1 and 2, it can be inferred that (i) a large fuel−water interfacial area is created when diesel or biodiesel−diesel blend (nonpolar liquid) is homogenized or mixed with water (polar liquid) as a result of the formation of larger number of tiny water drops, and (ii) the surfactant molecules adsorb readily to the newly created fuel−water interface, leading to the formation of water-in-fuel nEs. However, the stability of the water-in-fuel nEs formed is found to depend strongly on the concentration of biodiesel in the fuel blend. The kinetic stability of the diesel−water nEs stabilized by Span 80 and Tween 80 mixture (5% water, 85% diesel, and 5 vol % each surfactant) is found to be superior compared to the stability of biodiesel/diesel blend fuel emulsions formulated under similar water−fuel−surfactant composition and experimental conditions. The size of water drops in the nE fuels with 5−15% biodiesel (B5-nE, B10-nE, and B15-nE) is found to increase gradually with storage time, although no physical phase separation is observed. However, when the biodiesel concentration is further increased, B20-nE and B25-nE showed macroscopic and visible phase separation. Therefore, a combination of Span 80 and Tween 80 surfactants from water-in-fuel emulsions with limited stability is used, especially when the concentration of biodiesel in the fuel blend is higher than 20% by volume. The change in stability behavior may possibly due to change in (i) the molecular organization and packing of surfactant molecules and (ii) the adsorption/

https://doi.org/10.1021/acsomega.2c04711
ACS Omega 2022, 7, 44762−44771

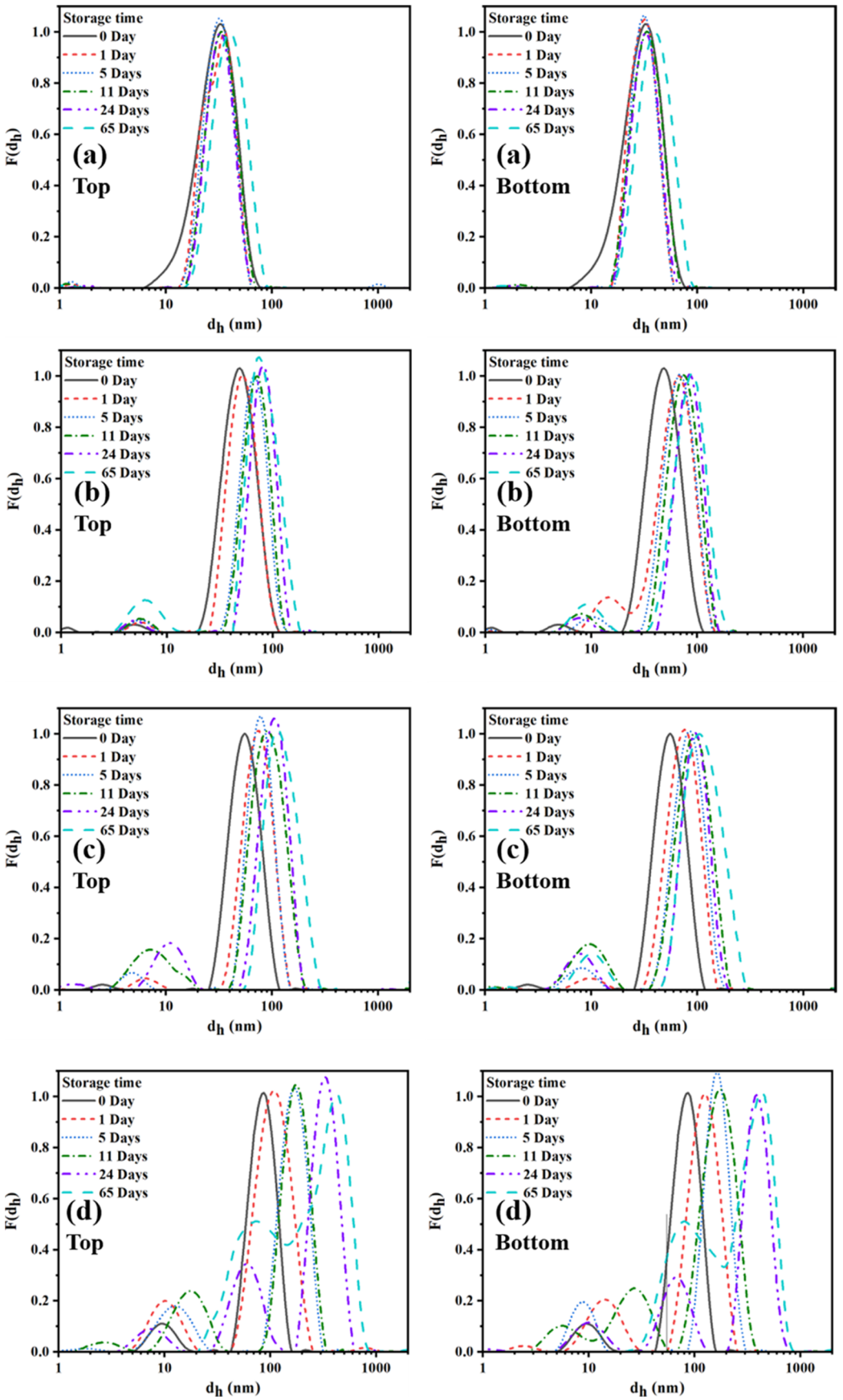

Figure 2. continued

https://doi.org/10.1021/acsomega.2c04711
ACS Omega 2022, 7, 44762−44771

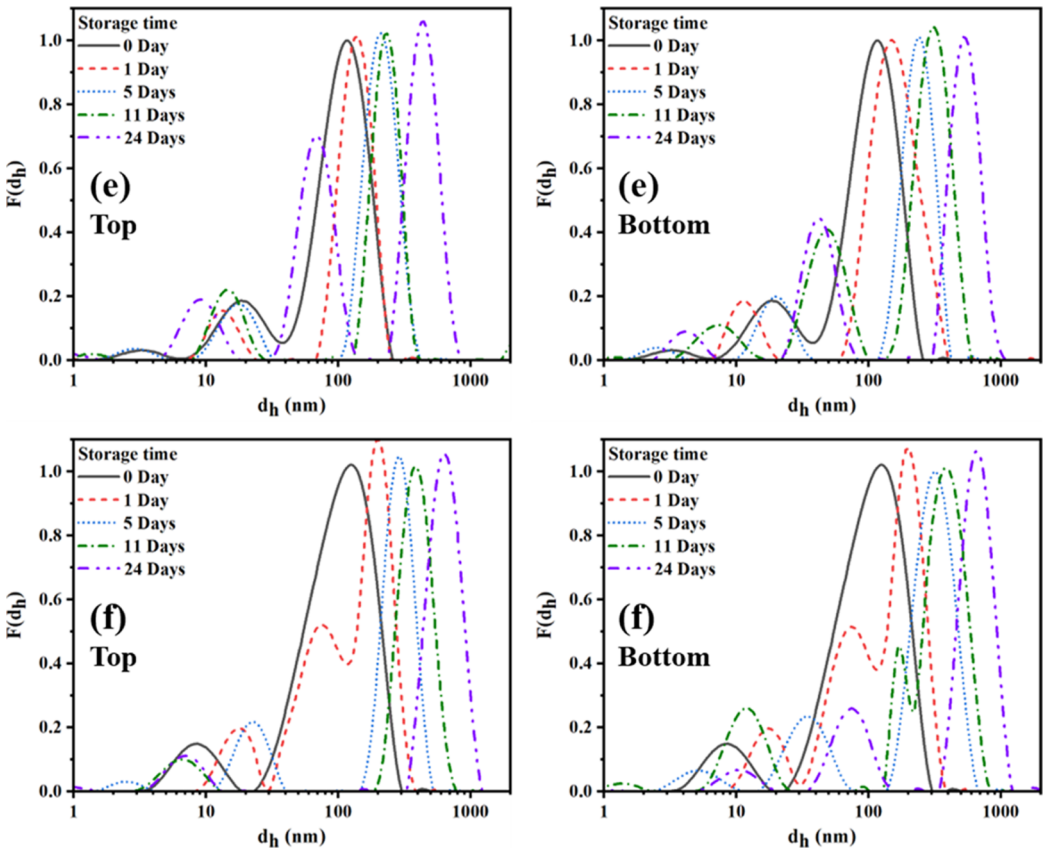

Figure 2. DSD obtained from CONTIN analysis (a: B0-nE, b: B5-nE, c: B10-nE, d: B15-nE, e: B20-nE, and f: B25-nE). Left DSD: top of storage vial and right DSD: bottom of storage vial.

desorption of surfactant molecules from the fuel−water interface. This calls for design of novel surfactants that are better suited for the development of diesel−biodiesel blend fuel emulsions that possess enhanced kinetic stability or may even be thermodynamically stable.

In the analysis that will follow, we will mainly focus on the temporal evolution of larger-sized drops, that is, higher peaks in the DSD. The droplet size in B15-nE increases to double (85−170 nm) in the first 5 days (Figure 2d). No significant change the in mean size is observed for the next 6 days. However, mean size increases to 420 nm, and bimodal distribution is prominent after total storage of 65 days. Similarly, for B20-nE and B25-nE, droplet size drastically evolved over aging, as shown in Figure 2e,f. For these two samples, the average droplet size increased by about an order of magnitude to 1000 nm within 24 days. As discussed earlier, B20-nE and B25-nE samples show phase separation and become destabilized after 65 days; hence, size distribution could not be obtained. Therefore, B0-nE, B5-nE, and B10-nE can be considered as highly stable due to negligible droplet size evolution over a sufficiently long storage period.

3.3. Change in Viscosity of Emulsified Fuels with Aging. The viscosity of emulsified fuels is typically higher than the viscosity of the base fluids used for emulsification. However, if the viscosity increases significantly, the emulsified fuels exhibit poor flowability, and hence such fuels are not favorable for engine applications. The ZSV is an important parameter determining the suitability of emulsified fuels for engine applications when they are formulated. The variation of ZSV of the emulsified fuels during long-term storage is also equally important as emulsions are prone to phase separation, creaming, and sedimentation. The viscosity measured at negligibly low shear rates can be considered as the viscosity of the emulsified fuel at rest. A higher ZSV also imparts additional kinetic stability as it impacts drop−drop coalescence. Hence, a study on the evolution of ZSV with storage time helps determine the shelf-life of the emulsified fuels. The relative ZSV of the emulsified fuels, which is defined as the ratio of ZSV of emulsified fuel to ZSV of continuous phase as a function of storage time, is shown in Figure 3. The dynamic

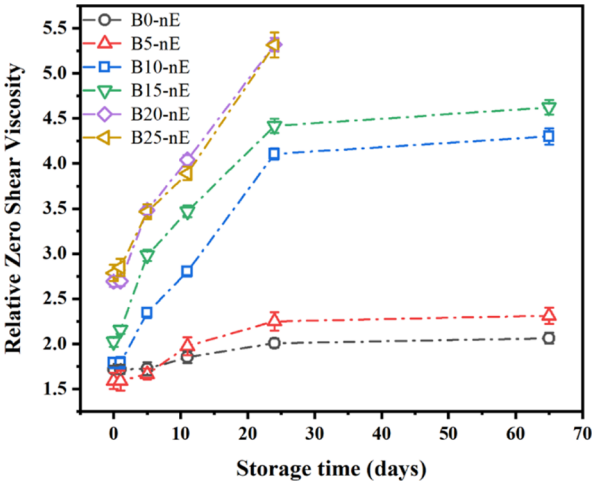

Figure 3. Temporal evolution of relative ZSV of emulsified fuels (lines are drawn as a guide to the eye).

https://doi.org/10.1021/acsomega.2c04711
ACS Omega 2022, 7, 44762−44771

viscosity of the emulsified fuel measured using a micro viscometer at three different inclination angles (around 20, 40, and 75°), which corresponds to measurements at three different shear rates, is extrapolated to obtain ZSV. The change in slope of the lines connecting the experimental points in Figure 3 is qualitatively related to the stability of the emulsified fuels. If no physicochemical changes occur in the emulsified fuels, the viscosity must ideally remain constant throughout the storage period. The relative ZSV of B0-nE is almost constant for the initial 6 storage days and does not change appreciably upon storage for 65 days. A nearly similar pattern is also observed for B5-nE. Although no change in relative ZSV is observed in B10-nE upon 1-day storage, it significantly increased by a factor of 2 when stored for 65 days. Nearly similar behavior is observed for B15-nE, with the relative ZSV increasing by a factor of 2 over 24 storage days. Thereafter, the relative ZSV is found to remain constant, indicating no further chemical or physical changes in the nE sample. The relative ZSV of B20-nE and B25-nE is found to change at almost the same rate from the first day and double within 24 days, similar to the B15-nE. However, B20-nE and B25-nE became unstable after 65 days, and relative ZSV could not be measured. Hence, it can be inferred from the relative ZSV data that B0-nE and B5-nE are the most stable emulsified fuels. The stability of emulsified fuel decreases as the biodiesel concentration increases due to physicochemical changes to the emulsified fuels occurring in B10-nE, B15-nE, B20-nE, and B25-nE.

3.4. Effect of Storage Temperature on the Stability of Emulsified Fuels. The storage temperature can significantly affect the stability of the nEs. Elevated temperature leads to rapid coalescence and simultaneous sedimentation or creaming of the droplets.[4] Hence, kinetically stable nEs are prone to phase separation when stored at a higher temperature. In this section, the stability of emulsified fuels at higher temperatures is assessed by observing the changes in the physical properties of the emulsified fuels.

3.4.1. Change in Density of Emulsified Fuels. Typically, density is inversely proportional to the temperature.[29] That is, density decreases with an increase in temperature. The density of the emulsified fuels as a function of temperature is shown in Figure 4. As the density of biodiesel is slightly higher than diesel, the density of the emulsified fuels increases with the increasing biodiesel concentration at all temperatures. Density decreases linearly with increasing temperature. However, the density of the emulsified fuels decreased marginally by 2.5% after increasing the storage temperature from 20 to 50 °C.

3.4.2. Change in Viscosity of Emulsified Fuels. The viscosity of the emulsions is expected to decrease with an increase in temperature. The ZSV of the emulsified fuels at different storage temperatures is shown in Figure 5. The viscosity of the samples gradually decreases with an increase in temperature except for B20-nE and B25-nE. Relatively, a sharp decrease in viscosity is observed for B20-nE and B25-nE, as evident from the higher slope of ZSV versus T plot. Since the viscosity of biodiesel is more affected by temperature than conventional diesel fuel,[9] the influence of temperature on the viscosity of emulsified fuels is more prominent for higher biodiesel concentrations.

3.4.3. Change in the Mean Droplet Size in Emulsified Fuels. The mean size of the droplets in the emulsified fuels as a function of storage temperature is shown in Figure 6. The

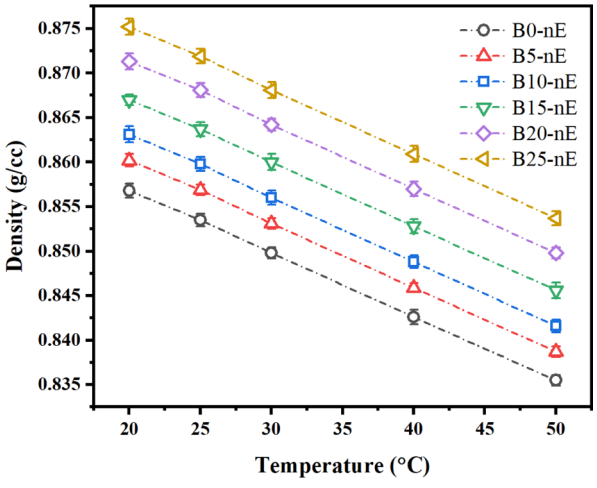

Figure 4. Variation in density of emulsified fuels with storage temperature (lines are drawn as a guide to the eye).

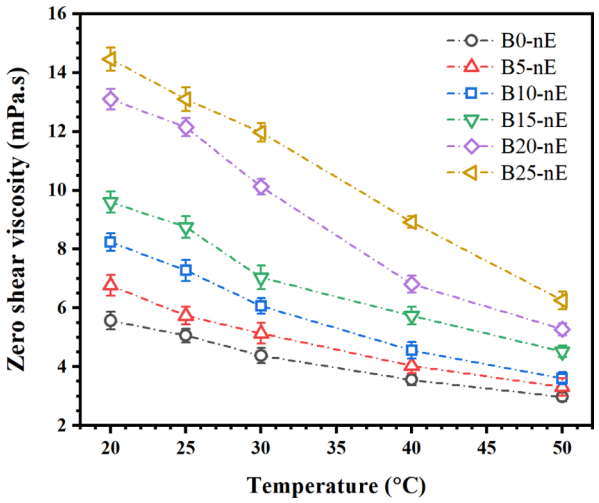

Figure 5. ZSV of emulsified fuels at different storage temperatures (lines are drawn as a guide to the eye).

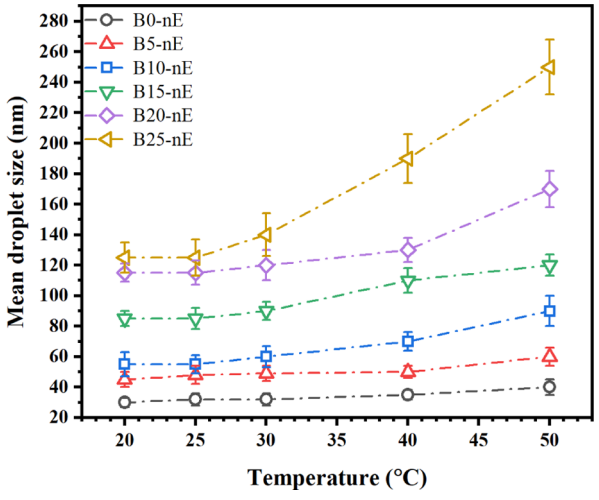

Figure 6. Change in the mean size of droplets in the emulsified fuels with temperature (lines are drawn as a guide to the eye).

https://doi.org/10.1021/acsomega.2c04711
ACS Omega 2022, 7, 44762−44771

droplet size does not change upon heating the samples from 20 to 25 °C. It is also evident that the elevated temperatures do not significantly affect the droplet sizes of B0-nE and B5-nE. Overall, the mean droplet size is increased by 33% in both samples when the temperature is increased from 20 to 50 °C. A significantly more change in the mean size was observed for B10-nE, B15-nE, and B20-nE at temperatures ranging from 30 to 50 °C. The mean droplet size of B25-nE almost doubled from 125 to 250 nm upon increasing the storage temperature from 20 to 50 °C. These observations suggest that blending more than 20% of biodiesel for preparing stable emulsified fuels has to be avoided, especially when the storage temperature is more than 30 °C.

4. CONCLUSIONS

A simple and effective method for preparing kinetically stable water in diesel and diesel/biodiesel blend nEs is presented. nE fuels with 5 vol % water, 10 vol % of an equi-volume mixture of Span 80 and Tween 80, and 85 vol % diesel/biodiesel blends are formulated. The biodiesel concentration in blend fuel varied from 0 to 25 vol %. First, the storage stability of nEs is investigated for a duration of 65 days at room temperature (25 °C) by monitoring the changes in the droplet size and relative ZSV. All samples except B20-nE and B25-nE are found to be macroscopically stable due to the absence of visually observable phase separation. The thermal stability of emulsion fuels is studied by storing the samples at elevated temperatures up to 50 °C. The emulsions are found to be stable within this temperature range with a moderate change in the ZSV, density, and mean droplet size. The temporal evolution of the DSDs of the nEs is measured with the help of DLS by performing CONTIN analysis. Droplet size analysis showed that extremely stable nE is formed when 85 vol % pure diesel is emulsified with 5 vol % water and 10 vol % equi-volume Span 80−Tween 80 mixture. No significant change in the droplet size and viscosity is observed even after 65 storage days. B5-nE and B10-nE are found to be moderately stable as the droplet sizes increased slightly. However, droplet sizes severely increase upon storage at higher biodiesel concentrations (i.e., B15-nE, B20-NE, and B25-nE). Thus, B0-nE, B5-nE, and B10-nE are recommended as possible alternative fuels based on their excellent long-time storage stability.

AUTHOR INFORMATION

Corresponding Authors

Niket S. Kaisare − *Department of Chemical Engineering, Indian Institute of Technology Madras, Chennai 600036, India;* orcid.org/0000-0001-9395-8784; Email: nkaisare@iitm.ac.in

Madivala G. Basavaraj − *Department of Chemical Engineering, Indian Institute of Technology Madras, Chennai 600036, India;* orcid.org/0000-0002-8275-5671; Email: basa@iitm.ac.in

Authors

Nitai C. Maji − *Department of Chemical Engineering, Indian Institute of Technology Madras, Chennai 600036, India; Department of Chemical Engineering and Technology, Indian Institute of Technology (BHU), Varanasi 221005, India*

Preetika Rastogi − *Department of Chemical Engineering, Indian Institute of Technology Madras, Chennai 600036, India*

Anand Krishnasamy − *Department of Mechanical Engineering, Indian Institute of Technology Madras, Chennai 600036, India;* orcid.org/0000-0001-7848-6213

Indrapal Singh Aidhen − *Department of Chemistry, Indian Institute of Technology Madras, Chennai 600036, India*

Complete contact information is available at: https://pubs.acs.org/10.1021/acsomega.2c04711

Notes

The authors declare no competing financial interest.

ACKNOWLEDGMENTS

The authors would like to express their gratitude to DST-SERB, Government of India (project no. CRG/2019/005732) and Institute postdoctoral fellowship of IIT Madras for their financial support. The authors are grateful to Professor Vinu Ravikrishnan, Chemical Engineering, IIT Madras, for helping with GC/MS analysis and HHV measurements of the fuel samples.

REFERENCES

(1) Leevijit, T.; Prateepchaikul, G.; Maliwan, K.; Mompiboon, P.; Eiadtrong, S. Comparative Properties and Utilization of Un-Preheated Degummed/Esterified Mixed Crude Palm Oil-Diesel Blends in an Agricultural Engine. *Renew. Energy* **2017**, *101*, 82−89.

(2) Popa, G.; Gheţi, M. A. Locomotive Diesel Engine Operation with Optimal Specific Fuel Consumption. *Procedia Manuf.* **2020**, *46*, 440−444.

(3) Sartomo, A.; Santoso, B.; Muraza, O. Recent Progress on Mixing Technology for Water-Emulsion Fuel: A Review. *Energy Convers. Manag.* **2020**, *213*, 112817.

(4) Maawa, W. N.; Mamat, R.; Najafi, G.; De Goey, L. P. H. Performance, Combustion, and Emission Characteristics of a CI Engine Fueled with Emulsified Diesel-Biodiesel Blends at Different Water Contents. *Fuel* **2020**, *267*, 117265.

(5) Chen, H.; Xie, B.; Ma, J.; Chen, Y. NOx Emission of Biodiesel Compared to Diesel: Higher or Lower? *Appl. Therm. Eng.* **2018**, *137*, 584−593.

(6) Gongora, B.; de Souza, S. N. M.; Bassegio, D.; Santos, R. F.; Siqueira, J. A. C.; Baricatti, R. A.; Gurgacz, F.; Secco, D.; Tokura, L. K.; Sequinel, R. Comparison of Emissions and Engine Performance of Safflower and Commercial Biodiesels. *Ind. Crops Prod.* **2022**, *179*, 114680.

(7) Elsanusi, O. A.; Roy, M. M.; Sidhu, M. S. Experimental Investigation on a Diesel Engine Fueled by Diesel-Biodiesel Blends and Their Emulsions at Various Engine Operating Conditions. *Appl. Energy* **2017**, *203*, 582−593.

(8) Patidar, S. K.; Raheman, H. Performance and Durability Analysis of a Single-Cylinder Direct Injection Diesel Engine Operated with Water Emulsified Biodiesel-Diesel Fuel Blend. *Fuel* **2020**, *273*, 117779.

(9) Phasukarratchai, N. Phase Behavior and Biofuel Properties of Waste Cooking Oil-Alcohol-Diesel Blending in Microemulsion Form. *Fuel* **2019**, *243*, 125−132.

(10) Gopidesi, R. K.; Rajaram, P. S. A Review on Emulsified Fuels and Their Application in Diesel Engine. *Int. J. Ambient Energy* **2019**, *43*, 732−740.

(11) McClements, D. J. Nanoemulsions versus Microemulsions: Terminology, Differences, and Similarities. *Soft Matter* **2012**, *8*, 1719−1729.

(12) Liang, J.; Qian, Y.; Yuan, X.; Leng, L.; Zeng, G.; Jiang, L.; Shao, J.; Luo, Y.; Ding, X.; Yang, Z.; Li, X. Span80/Tween80 Stabilized Bio-Oil-in-Diesel Microemulsion: Formation and Combustion. *Renew. Energy* **2018**, *126*, 774−782.

(13) Abdollahi, M.; Ghobadian, B.; Najafi, G.; Hoseini, S. S.; Mofijur, M.; Mazlan, M. Impact of Water − Biodiesel − Diesel Nano-

https://doi.org/10.1021/acsomega.2c04711
ACS Omega 2022, 7, 44762−44771

Emulsion Fuel on Performance Parameters and Diesel Engine Emission. *Fuel* **2020**, *280*, 118576.
(14) Basha, J. S.; Anand, R. B. An Experimental Study in a CI Engine Using Nanoadditive Blended Water-Diesel Emulsion Fuel. *Int. J. Green Energy* **2011**, *8*, 332−348.
(15) Rastogi, P.; Mehta, P. S.; Kaisare, N. S.; Basavaraj, M. G. Kinetic Stability of Surfactant Stabilized Water-in-Diesel Emulsion Fuels. *Fuel* **2019**, *236*, 1415−1422.
(16) Rastogi, P.; Kaisare, N. S.; Basavaraj, M. G. Diesel Emulsion Fuels with Ultralong Stability. *Energy Fuel.* **2019**, *33*, 12227−12235.
(17) Christensen, E.; McCormick, R. L. Long-Term Storage Stability of Biodiesel and Biodiesel Blends. *Fuel Process. Technol.* **2014**, *128*, 339−348.
(18) Kassem, M. G. A.; Ahmed, A. M. M.; Abdel-Rahman, H. H.; Moustafa, A. H. E. Use of Span 80 and Tween 80 for Blending Gasoline and Alcohol in Spark Ignition Engines. *Energy Rep.* **2019**, *5*, 221−230.
(19) Frisken, B. J. Revisiting the Method of Cumulants for the Analysis of Dynamic Light-Scattering Data. *Appl. Opt.* **2001**, *40*, 4087.
(20) Hassan, P. A.; Rana, S.; Verma, G. Making Sense of Brownian Motion: Colloid Characterization by Dynamic Light Scattering. *Langmuir* **2015**, *31*, 3−12.
(21) Provencher, S. W. Contin: A General Purpose Constrainded Regularization Program for Inverting Noisy Linear Algebraic and Integral Equations. *Comput. Phys. Commun.* **1982**, *27*, 229−242.
(22) Scotti, A.; Liu, W.; Hyatt, J. S.; Herman, E. S.; Choi, H. S.; Kim, J. W.; Lyon, L. A.; Gasser, U.; Fernandez-Nieves, A. The CONTIN Algorithm and Its Application to Determine the Size Distribution of Microgel Suspensions. *J. Chem. Phys.* **2015**, *142*, 234905.
(23) Marino, I.-G.Rilt MATLAB Central File Exchange. 2022, https://www.mathworks.com (Accessed 16 January 2022).
(24) Farbod, M.; Kouhpeymaniasl, R.; abadi, A. R. N. Morphology Dependence of Thermal and Rheological Properties of Oil-Based Nanofluids of CuO Nanostructures. *Colloids Surf. A Physicochem. Eng. Asp.* **2015**, *474*, 71−75.
(25) Dey, P.; Ray, S.; Newar, A. Defining a Waste Vegetable Oil-Biodiesel Based Diesel Substitute Blend Fuel by Response Surface Optimization of Density and Calorific Value. *Fuel* **2021**, *283*, 118978.
(26) Porras, M.; Solans, C.; González, C.; Martínez, A.; Guinart, A.; Gutiérrez, J. M. Studies of Formation of W/O Nano-Emulsions. *Colloids Surf. A Physicochem. Eng. Asp.* **2004**, *249*, 115−118.
(27) Leong, T. S. H.; Wooster, T. J.; Kentish, S. E.; Ashokkumar, M. Minimising Oil Droplet Size Using Ultrasonic Emulsification. *Ultrason. Sonochem.* **2009**, *16*, 721−727.
(28) van Kopanichuk, I.; Vedenchuk, E. A.; Koneva, A. S.; Vanin, A. A. Structural Properties of Span 80/Tween 80 Reverse Micelles by Molecular Dynamics Simulations. *J. Phys. Chem. B* **2018**, *122*, 8047−8055.
(29) Vasistha, V.; Bharj, R. S. Analyzing the Storage Stability of Diesel Emulsified Fuels: A Comparative Standpoint. *Energy Sources, Part A* **2022**, *44*, 5527−5544.

https://doi.org/10.1021/acsomega.2c04711
ACS Omega 2022, 7, 44762−44771